Development and Application of the Multipurpose Optical Flow Cell under Supercritical Condition of Water

Tomotsumi Fujisawa[1], Emi Maru[1], Fujitsugu Amita[1], Masafumi Harada[2], Tomoya Uruga[3], and Yoshifumi Kimura[4*]

[1]Department of Chemistry, Graduate School of Science, Kyoto University, Kyoto, 606-8502, Japan
[2]Department of Textile and Apparel Science, Faculty of Human Life and Environment, Nara Women's University, Nara 630-8506, Japan
[3]Japan Synchrotron Radiation Research Institute, 1-1-1, Kouto, Mikazuki-cho, Sayo-gun, Hyogo 679-5198, Japan
[4]Division of Research Initiatives, International Innovation Center, Kyoto University, Kyoto, 606-8501, Japan
[*]E-mail: ykimura@iic.kyoto-u.ac.jp

We have developed a new high-pressure and high-temperature optical cell which can be used under the flow condition. The window of the cell has a large aperture enough to be applicable to various kinds of laser and X-ray spectroscopy. The cell can be used up to 400 ºC and 40 MPa. As a demonstration, we applied the high pressure optical system to the measurement of the extended X-ray absorption fine structure (EXAFS) of cobalt(II) bromide ($CoBr_2$) aqueous solution under the sub- and supercritical condition. There is a large change in the Co K-edge EXAFS from 300 ºC to 380 ºC. The analysis of EXAFS suggests that the coordination number of water around cobalt ion reduces and that ion pairing with bromide ion increases.

1. Introduction

Various kinds of high pressure optical cells have been developed until now in order to apply laser spectroscopy and X-ray spectroscopy in high pressure fluids[1], since these spectroscopic methods are quite useful to extract various kinds of molecular interactions, molecular dynamics, and reaction dynamics in fluids. We have also developed various kinds of high pressure optical cells for laser spectroscopic measurements in supercritical fluids at the demand of each spectroscopic method, such as the transient absorption, time-resolved fluorescence, transient grating method, and so on[2-5].

In applying the laser spectroscopy to the high pressure fluid, the design of the optical window has a crucial importance in order to satisfy requirements of various optical alignments of the incoming and outgoing laser beams. Generally a large aperture of the optical window is required, which conflicts with the design standing the high pressure. In this paper, we present a new optical flow cell for high-pressure and high-temperature fluids including supercritical water, which is applicable to various spectroscopic methods such as the resonance Raman, transient grating, and X-ray absorption and diffraction spectroscopy. We aimed at the compact design of the cell and tried to improve the usability of the high-temperature and high-pressure optical cell.

By using this new developed optical cell, we demonstrate measurements of extended X-ray absorption fine structure (EXAFS) in sub- and supercritical water. Solvation of ions in supercritical water attracts much attention of a lot of chemists. Since EXAFS can approach the coordination structure around ion species, this method has been applied to ions in supercritical water from the earlier stage of researches on supercritical water[6-20]. Until now, the coordination structure around several ion species, such as strontium[6], rubidium[8,9,18], bromide[11,18], nickel[12], indium[14], copper[15], zinc[19], and so on, have been studied well. In this paper we have measured the EXAFS spectrum of cobalt (Co) K-edge EXAFS at different temperatures and pressures of cobalt(II) bromide ($CoBr_2$) aqueous solution. Kajimoto et al. have measured the pressure and temperature dependence of the d-d absorption spectrum of Co^{2+} in sub- and supercritical water[21]. Under the ambient condition, $CoBr_2$ is dissolved in water as $[Co(H_2O)_6]^{2+}$, and shows very weak absorption

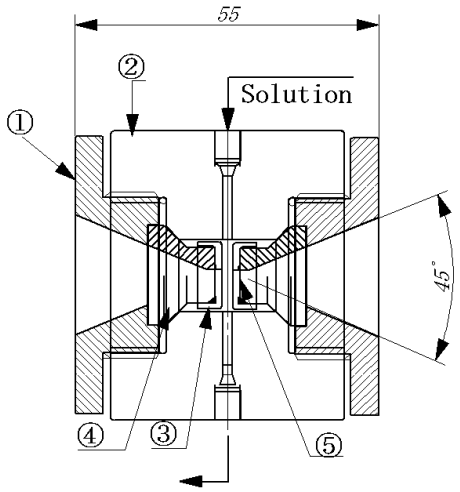

Fig. 1. Cross section of a high-pressure and high-temperature optical cell. ①Window support screw. ②Cell body. ③Window screw cap. ④Window support. ⑤Diamond window.

around 510 nm. However with increasing temperature, the absorption band shape shows a drastic change from 300 ºC to 400 ºC at 40 MPa; the peak position shifts to 670 nm, and the extinction coefficient is enlarged by more than twenty times. They interpreted the results as the consequence of the coordination structure changes from the octahedral to the tetrahedral. Our EXAFS analysis suggests that the coordination number of water around cobalt ion reduces in accordance with the change of the absorption spectrum of cobalt ion.

2. Experimental Methods

2.1. High pressure optical cell Figure 1 shows the cross section of a high pressure and high temperature optical cell. The basic design of the cell was similar to that in ref. 22. The cell body was made of SUS316 and was equipped with two optical windows. As a material of the window, synthesized diamond (Sumitomo Denko Type II a or Type Ib; diameter: 3.5 mm thickness: 0.5 mm) was used. The diamond window was pressed on a surface of a window support by a screw cap, where we used gold foil (thickness of 0.02 mm) as a gasket between the window and its support. By reducing the thickness of the window, we can get a large aperture of the optical window (ca. 45º) which is enough for the non-linear laser spectroscopy and

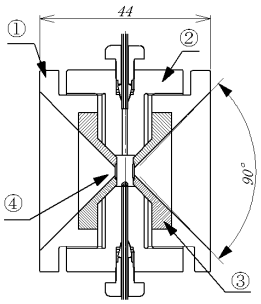

Fig. 2. Cross section of a wider aperture high-pressure and high-temperature optical cell. ① Window support screw. ②Cell body. ③Window support. ④Diamond window.

scattering experiments. The optical path length was 2 mm, and the bore of the window was 2 mm diameter. The material of the window support was hastelloy C. The seal between the cell body and the window support was attained by the line contact pressed by the screw. This cell could be used up to 400 ºC and 40 MPa.

Although the pressure seal stability became worse, much larger aperture size (90º) of the optical window was also available by using another type of the cell (Fig. 2). In this cell, the diamond widow was simply placed on the optical flat surface of the window. In order to get the initial seal, we used a glue to attach the diamond window to the window

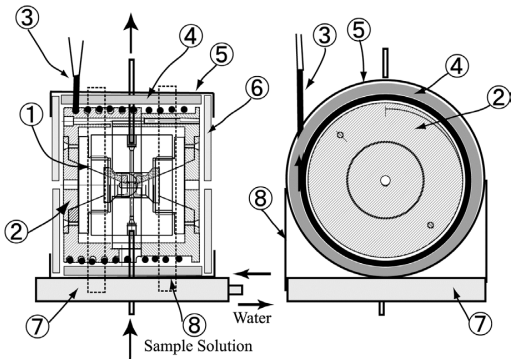

Fig. 3. Schematic drawings (side cross section and front view) of a heating system of the high pressure optical cell. ① High pressure optical cell. ② Heating jacket. ③ Sheathed heater. ④ Rock wool. ⑤ Stainless steel container. ⑥ Heat insulator. ⑦ Stage. ⑧ Band. In the front view, the heat insulator is omitted.

support. Another merit of using this cell was a minimum dead volume of the cell. The designs of the other parts were almost similar to those in Fig. 1. By using this window, we could control the system up to 300 ºC and 30 MPa.

Figure 3 shows a heating system of the high pressure optical cell. The temperature of the optical flow cell was monitored by a thermocouple inside the cell, and controlled by a sheathed heater (1kW) and a thermoregulator (OMRON E5CN). The optical cell was encapsulated in a jacket made of brass, and the sheathed heater was wound around the jacket. The brass jacket was wrapped by rock wool and fixed into a stainless steel container of cylindrical shape as is shown in Fig. 3. The optical bore sizes of the jacket and the heat insulator were adjustable according to the experimental methods used. The container was put on a stage made of stainless steel and fixed to the stage by a stainless steel band. Thermo-regulated water was flowed through inside the stage in order to prevent the heating of materials connected to the stage.

In using the system at the higher temperature under a flow condition, a pre-heater was required in order to keep high temperature inside the cell. As a pre-heater, we used a compact device which was composed of a high pressure tube and a sheathed heater wound around the heat transfer medium[23].

2.2. EXAFS measurements EXAFS measurements of Co K-edge of aqueous solution of $CoBr_2$ ($[Co^{2+}]$=50mM) were performed in a transmission mode at BL01B1 in SPring-8 (Japan Synchrotron Radiation Research Institute) using synchrotron radiation from 8 GeV storage ring. A schematic illustration of the system is shown in Fig. 4. The data were collected using ionization chambers filled with nitrogen for the incident intensity (I_0) and nitrogen/argon (75/25) for the transmitted intensity (I). The high pressure optical cell with the heating unit was placed on X and Z translational stages (Sigma Koki, STM-50X and STM-20ZF) and on a θ rotation stage (Suruga Seiki, K401-60) which are electronically driven in order to control the cell position to introduce the X-ray into the cell window at the correct position. The X-ray beam was squared shape of 1×1 mm^2.

In measuring the EXAFS spectrum, the sample solution was flowed at 1 or 0.5 cm^3 min^{-1}. The solution was pumped by a HPLC pump (JASCO Corp. PU-2080plus) and the system pressure was regulated by a back pressure regulator (JASCO Corp. 880-81). We applied a quick scan mode by

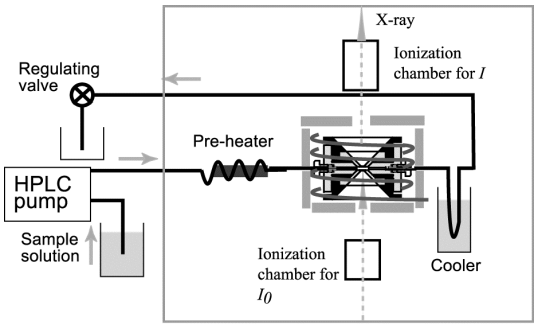

Fig. 4. Schematic drawing of a system for the EXAFS measurement.

which we can measure an X-ray absorption spectrum within short time duration (typically 10 to 20 min for the present measurements) with enough signal to noise (S/N) ratio. After the temperature and the pressure became stable under the flow condition of pure water, the background X-ray absorption was measured at first. Then the sample solution was flowed and the X-ray absorption of sample solution was measured after the solution inside the cell was well replaced. Again pure water was flowed through the cell, and the background absorption was re-measured. We repeated this procedure twice or three times, and checked the signal stability and averaged the spectra. At the high temperature condition, there was a very small edge jump for the background absorption due to the stain of the window after the following the cobalt solution. At present we are not sure of the origin of this. There may be some reaction between cobalt ion and oxygen dissolved in the water or other contamination from the cell material, which occurs on the surface of the window or the surface of the cell body. This effect may be reduced by degassing the sample solution before flow, or changing the material of the cell which is more tolerable for supercritical water.

2.3. EXAFS data analysis The detail of the EXAFS analysis is described elsewhere[24]. Briefly, the raw EXAFS data in energy space ($\log(I_0/I)$) vs. E, where E is the X-ray energy, were reduced to the photoelectron wave vector (k) space with the threshold energy E_0, where $k = [2m(E-E_0)/\hbar^2]^{1/2}$ ($\hbar = h/2\pi$ where h is the Planck constant). Since there was a very small edge jump for the background absorption due to the stain of the window at the high temperature conditions as is mentioned before,

we subtracted the background signal of pure water and the cell windows from the observed spectra for 350 ºC and 380 ºC. The EXAFS spectra for Co-K edge were extracted using a spline smoothing method[25] and normalized to the edge height. The $k^2\chi(k)$ function vs k data and the corresponding Fourier transforms were obtained using Hanning window function with 1/20 FT ranges. The typical range of Fourier transformation from the k space to the r space was 20-120 nm^{-1}. The EXAFS spectra were fitted by the following function,

$$k^3\chi(k) = \sum_j N_j F_j(k_j) k_j^{\,2} \exp(-2\sigma_j^{\,2} k_j^{\,2}) \times \sin[2k_j r_j + \phi_j(k_j)] / r_j^{\,2} \quad (1)$$

where

$$k_j = (k^2 - 2m\Delta E_{0j}/\hbar^2)^{1/2} \quad (2)$$

Here N_j denotes the coordination number, r_j the bond distance, ΔE_{0j} the difference between the theoretical and experimental threshold energies, and σ_j the Debye-Waller factor of the j-th coordination shell, respectively. The data were fitted with phase shift ($\phi_j(k)$) and amplitude functions ($F_j(k)$) by McKale[26] using the REX2000 software (Rigaku Corp.).

3. Results and Discussion

Figure 5 presents the Co K-edge k^2-weighted χ(k) plots at various temperatures for 50 mM $CoBr_2$ aqueous solutions. In all cases, the usable k-range extends to ~12 $Å^{-1}$. As is shown in the figure, the amplitude of the oscillation becomes small with an increase of the temperature, and the large change is observed above 350 ºC.

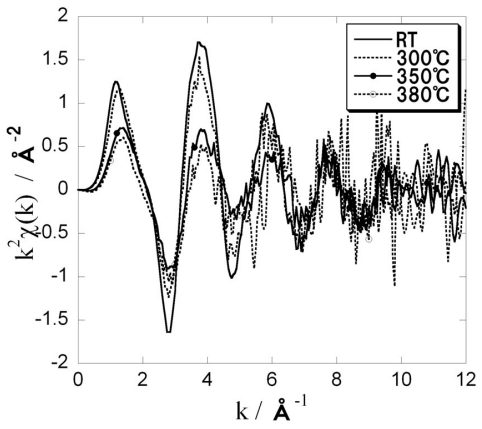

Fig. 5. The k^2-weighted $\chi(k)$ plots for Co K-edge EXAFS for aqueous solutions of $CoBr_2$ at various temperatures and pressures.

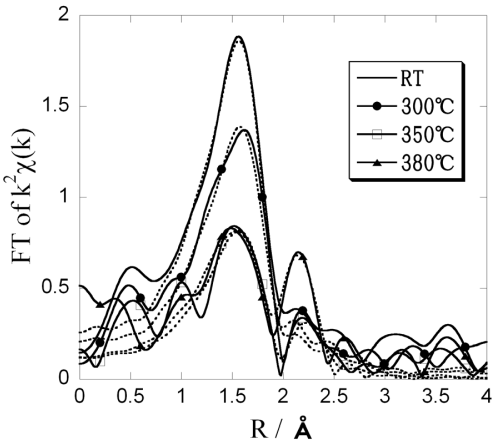

Fig. 6. The Fourier transform of $k^2\chi(k)$ for Co K-edge EXAFS for the aqueous solutions of $CoBr_2$ at various temperatures and pressures.

Figure 6 shows the corresponding Fourier transformed data. This figure illustrates the probability of finding a particular atom at a certain distance from the central scattering Co atom. The plot clearly indicates that the number of the nearest neighbor atoms (corresponding to the peak around 1.5 Å) decreases with increasing temperature, and another peak around 2.2 Å gradually increases above 350 ºC. The peaks which appear at the shorter distances than ~1 Å are due to an artifact arising from the Fourier transform of $k^2\chi(k)$ that mostly contains a residual contribution from the background function.

The dashed lines in Fig. 6 represent the results of the fit to Eq. (1). The data below 300 ºC were fit by a contribution of a single species (oxygen atom). On the other hand, at the higher temperatures (350 ºC and 380 ºC), including another atomic species (bromide) resulted in better results. The tabulated values of parameters obtained from this fitting are listed in Table 1. Under the ambient condition, it is known that Co^{2+} is in a octahedral form $[Co(H_2O)_6]^{2+}$. The bond distance is reported as 2.08 Å[27]. The bond distance estimated here matches the reported value well. The smaller coordination number (4.9) at the ambient condition is probably due to the imperfectness of the backscattering phase shift and amplitude function [$\phi(k)$ and $F(k)$] from the McKale and due to the

Table 1. Results of Co K-edge EXAFS analysis of first-shell Co^{2+} hydration and ion pairs with Br^- under liquid and supercritical conditions for the 0.05 M aqueous solution of $CoBr_2$. The estimated error of the coordination number (N_j) from the variation of Debye-Waller factor (σ, ±0.01) is ±0.5 at most.

T / ºC	P / MPa	d /g cm^{-3}	N_O	R_O/Å	σ_O / Å	N_{Br}	R_{Br}/Å	σ_{Br} / Å
25	30	1.01	4.9	2.07	0.076	–[a)]	–[a)]	–[a)]
300	30	0.75	4.0	2.08	0.078	–[a)]	–[a)]	–[a)]
350	20	0.60	2.0	2.04	0.074	1	2.43	0.1
380	40	0.59	2.1	2.05	0.087	1.8	2.40	0.085

[a)]Not detected.

multiple reflection contributions. Therefore the true coordination numbers of oxygen are 6/4.9 times of the values in the table. From room temperature to 300 ºC, the coordination number of the oxygen atom does not show a significant change. On the other hand, above 300 ºC, the coordination number of oxygen drastically decreases and bromide anion becomes to contribute to the spectrum. The bond distance between Co^{2+} and Br^- estimated here is close to the value reported for the case of Ni^{2+}[12], although the coordination numbers at the higher density have larger errors due to the poor S/N.

Our results strongly support the previous interpretation of the temperature dependence of the d-d absorption spectrum of Co^{2+} under the sub- and supercritical conditions of water. From 300 to 400 ºC at 40 MPa, the weak absorption band around 510 nm shifts to 670 nm and increases in its intensity. This was interpreted as the consequence of the coordination structure transition from $[Co(H_2O)]^{2+}$ to $[CoBr(H_2O)_3]^+$, $[CoBr_2(H_2O)_2]$, and $[CoBr_3(H_2O)]^-$ in SCW[21]. The changes of the coordination number obtained here quite well explain the observation of the UV-Vis absorption spectrum.

4. Conclusions

We have developed a high-pressure and high-temperature optical flow cell which has a large aperture of the optical window which can be used for the various kinds of laser and X-ray spectroscopy. As a demonstration, we have measured the Co K-edge EXAFS for the sub- and supercritical condition of aqueous solution of $CoBr_2$. We found that above 300 ºC, the coordination number of oxygen decreases and bromide anion contributes to the spectrum. Further consideration on the coordination structure is now progressing utilizing the analysis of the EXAFS by FEFF[28] programs. In the near future, we will apply the same optical system to the resonance Raman and transient grating spectroscopy for the high-temperature and high-pressure fluids.

Acknowledgements

This work is supported by the research program by SPring-8 (2002B0750-NX-np and 2004A0072-NXa-np). This work is partially supported by the fund from the Tokuyama Science Foundation.

References and Notes

[1] see e.g., W. F. Sherman and A. A. Stadtmuller, in *Experimental Techniques in High-Pressure Research,* John Wiley & Sons Ltd., Chichester, 1987.
[2] Y. Kimura, D. Kanda, M. Terazima, and N. Hirota, *Ber. Bunsenges. Phys. Chem*., **99**, 196 (1995).
[3] T. Yamaguchi, Y. Kimura, and N. Hirota, *J. Phys. Chem. A*, **101**, 9050 (1997).
[4] T. Ohmori, Y. Kimura, N. Hirota, and M. Terazima, *Phys. Chem. Chem. Phys.*, **3**, 3994 (2001).
[5] N. Saga, Y. Kimura, N. Hirota, and M. Terazima, *Analytical Sciences*, **17**, s234 (2001).
[6] D. M. Pfund, J. G. Darab, J. L. Fulton, and Y. Ma, *J. Phys. Chem*., **98**, 13102 (1994).
[7] K. Tamura, M. Inui, and S. Hosokawa, *Rev. Sci. Instrum.,* **66**, 1382 (1995).
[8] B. J. Palmer, D. M. Pfund, and J. L. Fulton, *J. Phys. Chem.*, **100**, 13393 (1996).
[9] J. L. Fulton, D. M. Pfund, S. L. Wallen, M. Newville, E. A. Stem, and Y. Ma, *J. Chem. Phys*., **105**, 2161 (1996).
[10] S. L. Wallen, D. M. Pfund, J. L. Fulton, C. R. Yonker, M. Newville, and Y. Ma, *Rev. Sci. Instrum*., **67**, 2843 (1996).
[11] S. L. Wallen, B. J. Palmer, D. M. Pfund, J. L. Fulton, M. Newville, Y. Ma, and E. A. Stern, *J. Phys. Chem. A*, **101**, 9632 (1997).
[12] M. M. Hoffmann, J. G. Darab, B. J. Palmer, and J. L. Fulton, *J. Phys. Chem. A*, **103**, 8471 (1999).

[13] M. M. Hoffmann, J. G. Darab, S. M. Heald, C. R. Yonker, and J. L. Fulton, *Chemical Geology*, **167**, 89 (2000).
[14] T. M. Seward, C. M. B. Henderson, and J. M. Charnock, *Chemical Geology*, **117**, 118 (2000).
[15] J. L. Fulton, M. M. Hoffmann, J. G. Darab, B. J. Palmer, and E. A. Stren, *J. Phys. Chem. A*, **104**, 11651 (2000).
[16] Y. Calzavara, V. Simonet, J. L. Hazemann, R. Argoud, O. Geaymond, and D. Raoux, *J. Synchrotron Rad*., **8**, 178 (2001)
[17] J. L. Fulton, J. G. Darab, and M. M. Hoffmann, *Rev. Sci. Instrum.*, **72**, 2117 (2001).
[18] G. Ferlat, A. San Miguel, J. F. Jal, J. C. Soetens, Ph. A. Bopp, I. Daniel, S. Guillot, J. L. Hazemann, and R. Argoud, *Rhys. Rev. B*, **63**, 134202 (2001).
[19] V. Simonet, Y. Calzavara, J. L. Hazemann, R. Argoud, O. Geaymond, and D. Raoux, *J. Chem. Phys*., **116**, 2997 (2002).
[20] J. L. Fulton, S. M. Heald, Y. S. Badyall, and J. M. Simonson, *J. Phys. Chem. A*. **107**, 4688 (2003).
[21] O. Kajimoto, E. Maru, and K. Okada, in preparation.
[22] F. Amita, K. Okada, H. Oka, and O. Kajimoto, *Rev. Sci. Instrum.,* **72**, 3605 (2001).
[23] F. Amita, H. Oka, M. Mukaide, Y. Urasaki, K. Takegoshi, T. Terao, and O. Kajimoto, *Rev. Sci. Instrum.,* **75**, 467 (2004).
[24] B. K. Teo, *EXAFS Basic Principles and Data Analysis*, Inorganic Chemistry Concepts, Vol. 9, Springer-Verlag, Berlin, 1986.
[25] J. W. Cook and D. E. Sayers, *J. Appl. Phys*., **52**, 5024 (1981).
[26] A. D. McKale, B. W. Veal, A. P. Pailikas, C. K. Chan, and G. S. Knapp, *J. Am. Chem. Soc*., **110**, 3764 (1988).
[27] Y. Inada, H. Hayashi, K. Sugimoto, and S. Funahashi, *J. Phys. Chem. A*, **103**, 1401 (1999).
[28] A. L. Ankudinov, B. Ravel, J. J. Rehr, and S. D. Conradson, *Phys. Rev. B*, **58**, 7565 (1998).